

ANALYSIS OF ANISOTROPIC VELOCITIES IN A CORE SAMPLE AND AVOA FROM A FRACTURED VUGGY CARBONATE RESERVOIR

Stephen A. Hall^{*}, Robert R. Kendall[†], J-Michael Kendall[‡] and Carl Sondergeld[§]

^{*}University of Leeds Now at Department of Petroleum Engineering, Heriot-Watt University, UK

[†] Amoco Production Company, New Orleans, USA, now at Veritas DGC, Calgary, Canada

[‡]School of Earth Sciences, University of Leeds, UK

[§] Amoco Production Company, Tulsa now at The University of Oklahoma, Tulsa, OK 74135

Abstract. We investigate the effects of fracture- and inclusion-induced seismic anisotropy in a carbonate reservoir rock and the resulting influence this anisotropy may have on surface seismic data. Whole-core velocity measurements made on a carbonate sample from the Gulf of Mexico show evidence of elastic anisotropy. Constraints on the style of this anisotropy are obtained from comparisons with effective medium modeling. The core exhibits monoclinic symmetry, which is interpreted as being caused by the combined effects of vertically-aligned drilling-induced fractures and oriented ellipsoidal vugs inclined at an angle roughly 60° to the vertical. The *in situ* anisotropy is believed to be orthorhombic, as there is evidence of natural fractures oriented orthogonally to the vugs. Surface seismic modeling is used to investigate amplitude variations with offset and azimuth (AVOA) effects due to such anisotropy. Our model is somewhat hypothetical, but consistent with velocities from the reservoir logs and the inferred *in situ* anisotropy. Our results suggest that for this model, P-wave AVOA will show significant azimuthal variation only at far offsets (near critical reflections). In fact, the onset of critical reflections will be dependent on the orientation of the seismic line with respect to the fracture direction. Shear modes will be more sensitive to fracture orientation at near offsets. In addition, we find that the P-P and P-S AVOA are sensitive to the presence of aligned vuggy porosity and so could provide a tool for identifying highly productive zones where fractures connect vugs.

1 Introduction

The detection of subsurface fracturing can be a key factor in deciding the economic potential of a reservoir, especially in situations of good porosity but poor permeability. The preferred alignment of such fractures produces seismic anisotropy (e.g., Crampin, 1993) which is detectable in both P-wave data [e.g., Lynn et al., 1996 (land data); Horne et al., 1997 (VSP data); MacBeth et al., 1999 (ocean-bottom data)] and shear-wave data (e.g., Mueller, 1991; Kendall and Kendall, 1996). The preferred alignment of ellipsoidal inclusions will also produce

a long-wavelength anisotropy; the limiting case of inclusions with infinite aspect ratio is equivalent to Backus (1962) layering. Here we consider the anisotropy of a fractured carbonate which contains preferentially aligned ellipsoidal vugs.

Whole-core velocity measurements were made on a carbonate sample from the Gulf of Mexico in order to characterize its heterogeneity and assess any anisotropy. We use an effective medium modeling approach to interpret the form and magnitude of the anisotropy in the core sample. It is not our intention to characterize the *in situ* anisotropy of the reservoir,

but rather our aim is to illustrate potential anisotropy due to aligned fractures and inclusions (vugs). The core observations also provide a means for testing the effective medium theory. Our final aim is to investigate the potential for using amplitude variations with offset and azimuth (AVOA) to identify productive regions characterized by aligned fractures and zones of oriented vuggy porosity. In a companion paper we more generally consider AVOA modeling for fractured media (Hall and Kendall, 2000, this issue).

The reservoir unit consists of a Cretaceous age massive carbonate from slope and deep water deposition. Certain intervals have been highly dolomitized through a deep reflux process, whereas other intervals, being only partially dolomitized, are predominantly limestone. The greatest production is from brecciated calcareous zones and intervals where fractures connect vugs. The breccia zone, at the top of the producing interval, has been exploited since the discovery of the field. However, vuggy zones provide significant hydrocarbon storage potential and are believed to form discrete layers that give the reservoir a distinctive layered-no-cross-flow behavior. The presence of natural fractures will greatly affect production rates, especially where they intersect the vuggy bands providing permeability pathways through the otherwise low permeability rock unit. Exploitation of these fractured vuggy zones could provide an extended tertiary recovery phase to the field, which is presently under water injection.

Figure 1 shows examples of thin sections from the cored interval, with natural fractures intersecting vuggy porosity. Figure 2 shows photographs of the core sample. Detailed observation of the core sample and thin sections show that the vuggy porosity is generally ellipsoidal in shape and aligned in linear bands. *In situ*, the vugs vary in size from millimeters to meters. Natural fractures intersect the vugs with an orientation perpendicular to that of the vug alignment. Both the natural fractures and the bands of vugs show some degree of late-stage recrystallization and oil-staining which differentiates them from

drilling-induced fractures which are also observed in thin sections. The drilling-induced fractures are aligned parallel to the axis of the core so, due to an inclined drilling direction, are not aligned with the vertically oriented naturally occurring fractures.

2 Whole core velocity measurements

Ultrasonic P- and S-velocity measurements were made at the Amoco EPTG Tulsa Rock Properties Lab on a whole core sample at room temperature, pressure and humidity (see <http://www.ou.edu/mewbourneschool/cfrp/ic3/cfrp.htm> for a description of the procedure). Figure 3 illustrates the different measurements that were made. Circumferential velocity analysis (CVA) of body waves traveling in the plane perpendicular to the core axis was done at the top, middle and bottom of the sample. P-wave CVA measurements were also made along a path oriented 45° to the core axis. Last, P-wave velocities were measured along the core axis.

An example of the data from the P-wave CVA measurements in a plane perpendicular to the core axis, at the middle of the sample, is shown in Figure 4(a). This figure shows clear first breaks and an obvious variation in traveltime around the circumference. A maximum traveltime is observed between about 150° and 160° azimuth. Figure 4(b) illustrates the variation in the velocity of the horizontally polarized shear-wave for the same configuration. It can be seen that the shear-wave first arrivals are of reduced data quality. Also, no attempt was made to rotate the shear-wave traces to their true fast and slow direction before picking arrivals. However, a velocity minimum is clearly evident from late arrivals in the region of the 150° azimuth. Figure 5 presents the core velocity data and shows clear evidence of anisotropy in the ultrasonic wave propagation through the sample.

The next sections describe how the elastic measurements of the core are combined with acoustic log

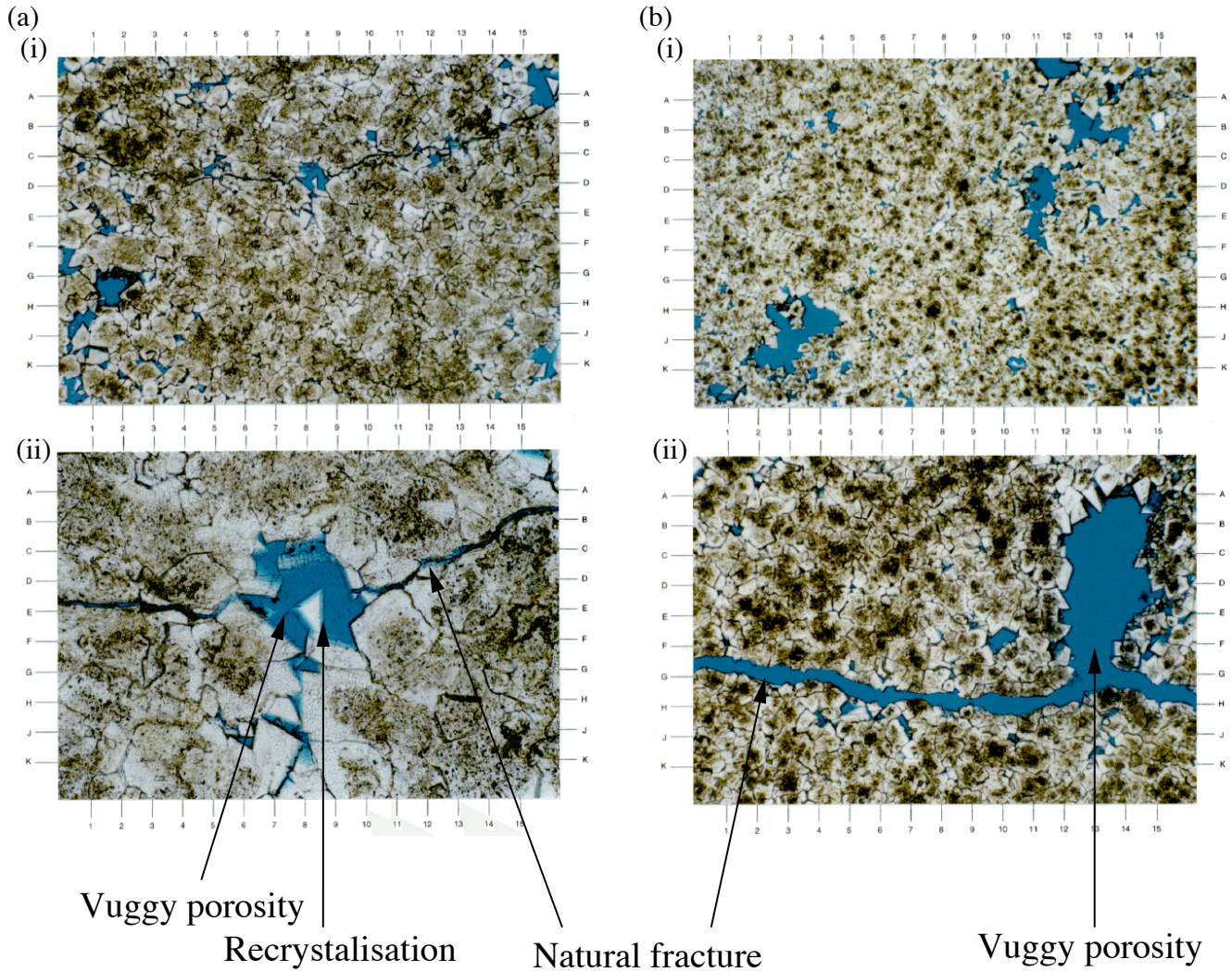


Figure 1: Examples of thin sections taken from the core sample; (a) (i) 31x magnification (ii) 125x magnification of a section of (i); (b) (i) 16x magnification, (ii) 31x magnification of a different area of the same section. Both sections show open (natural) micro-fractures intersecting vuggy porosity. Evidence of late stage recrystallisation in the vuggy pore space can also be seen.

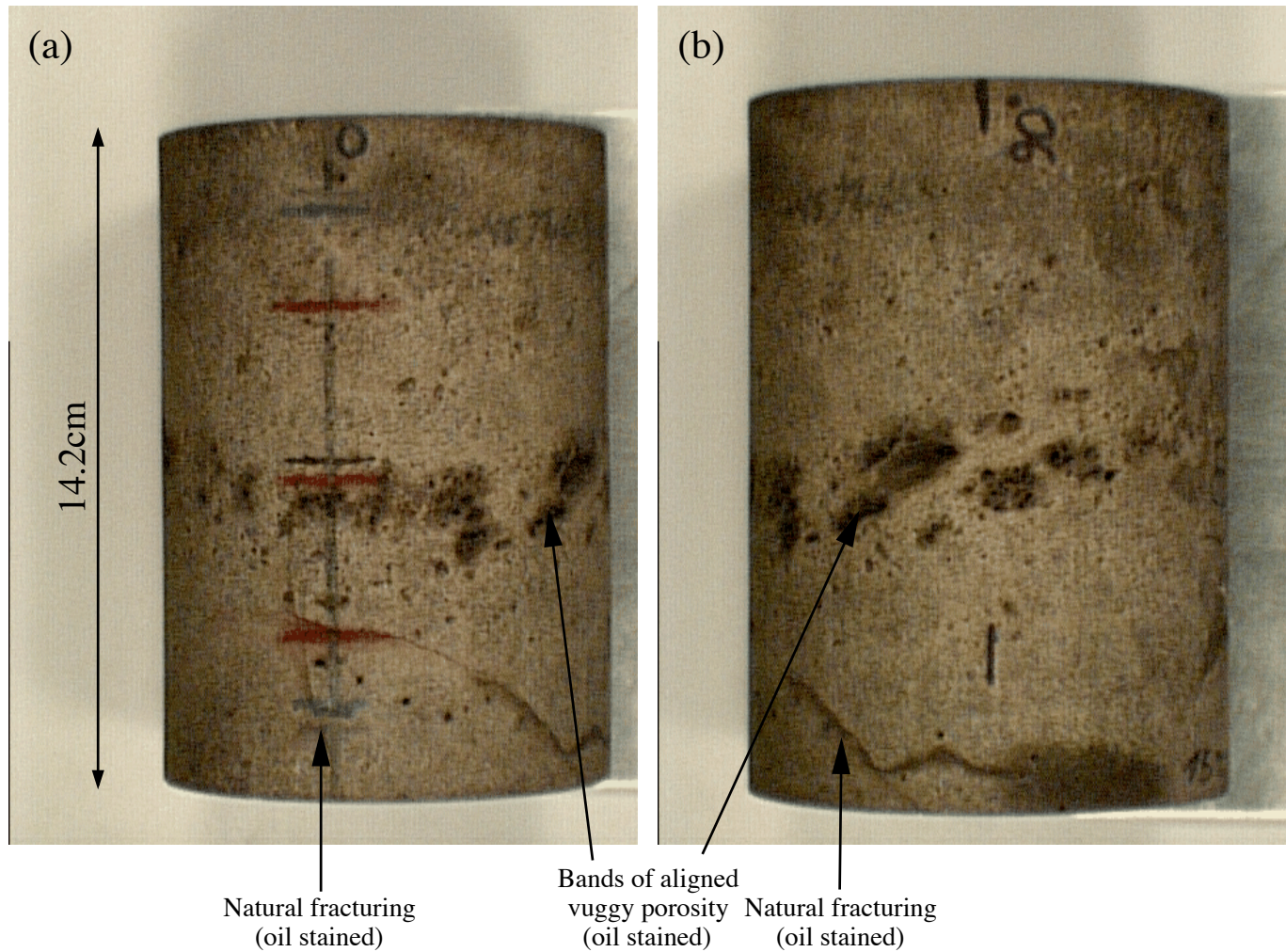


Figure 2: Photos of the core sample, (a) at 0° azimuth and (b) at 90° (anticlockwise) to (a). The red marks in (a) indicate the positions of the transducers for the ultrasonic measurements, see Figure 3. Vuggy porosity is seen in bands dipping from about 180° to 0° with some natural fracturing roughly orthogonal to the vug alignment. Both vugs and natural fractures are dark in colour due to oil-staining.

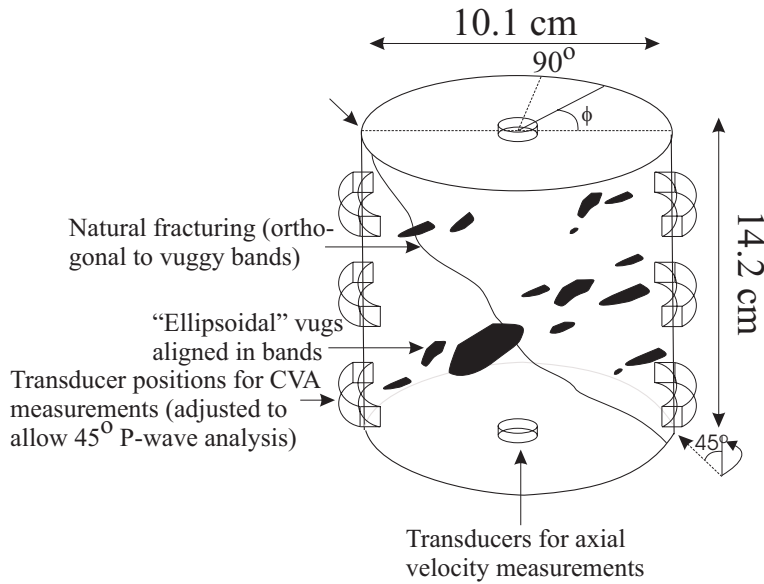


Figure 3: Diagram of the core sample showing the measurement configuration and a diagrammatic representation of the vuggy bands and natural fracturing. CVA measurements are made around the sample at the three positions indicated; see Figure 2. The transducer positions are adjusted for the 45° P-wave measurements.

and density log measurements to build an effective medium model of the core sample. As the core measurements are not made at *in situ* conditions, we note that the actual anisotropy within the reservoir will no doubt be different. A precise description of the reservoir anisotropy is not our intention, but rather we wish to explore the more generic effects of reservoir anisotropy due to aligned fracturing and intersecting zones of aligned vugs.

3 Modeling the response of the core

Effective medium modeling is used to describe the effective elasticity of the core sample with aligned fractures and/or vugs. The anisotropy of the core sample is constrained through comparison with a range of effective medium models. Modeled velocities are compared to the P-wave measurements to find the best-fit solution. The shear-wave measurements are used only as a loose constraint, since

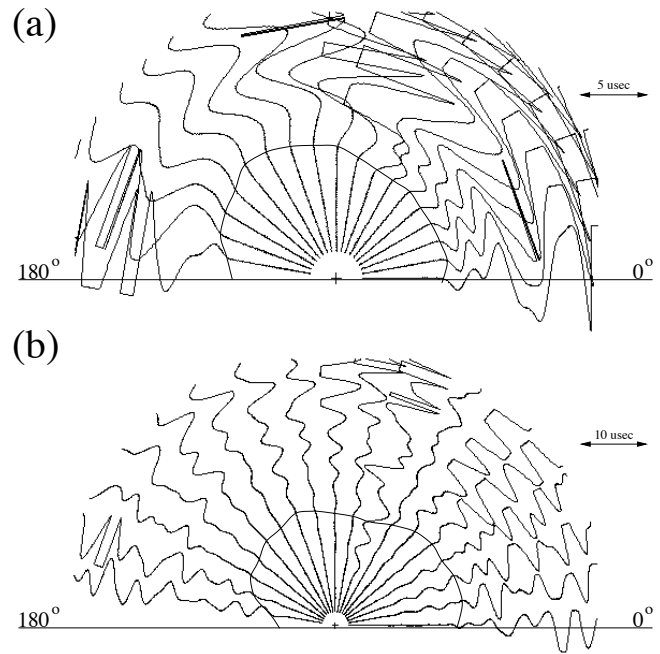


Figure 4: Time series for the CVA measurements at the middle position on the sample for the (a) P-waves and (b) S_h waves. Approximations for the first arrival picks are indicated.

they proved to be less reliable, as described earlier. Our method for effective medium modeling follows that of Schoenberg and Sayers (1995), but appeals to Hudson (1981) to calculate the additional compliance terms of the aligned fractures and vugs. Details of the effective medium modeling are given in the companion paper by Hall and Kendall (2000, this issue) and in Hall (2000).

Figure 5 shows velocities determined using different effective medium models based on features identified in the sample that can produce anisotropy (i.e., subhorizontally aligned vugs, natural fractures orthogonal to the vugs, and drilling-induced fractures parallel to the core axis). These modeled velocities are compared to the velocity measurements of the sample. In the models used, estimates of the fracture and vug characteristics are based on their combined porosity being 8%, as estimated from the log data. It was assumed that 10% of this porosity is due to fracturing. The core photo suggests an average aspect ratio for the vugs of 0.4 and gives a “crack-density” of 0.05. A range of crack densities and aspect ratios, consistent with the fracture porosity, was tested. The fractures and vugs were taken to be air-filled, as the sample was dry. The anisotropy due to each feature is assumed to be transverse isotropy with a variable symmetry axis and is modeled using the approach described in Hall and Kendall (2000). The isotropic P-wave velocity of the host rock was taken to be the fastest P-wave velocity measured in the sample. The isotropic S-wave velocity was the best-fit value constrained by typical V_p/V_s ratios in carbonates. The density of the rock frame was taken as the measured density of the carbonate grains.

The nature of the deviation of the CVA measurements from the isotropic case (see Figure 5) suggests that transverse isotropy (TI) with a symmetry axis aligned parallel to the axis of the core can be ruled out. Furthermore, the P-wave CVA measurements at all levels indicate a $\cos 2\phi$ velocity variation with azimuth ϕ , with faster velocities roughly around 30° . Such a variation could indicate a transversely isotropic medium with a symmetry axis perpendicu-

lar to the core axis and oriented along an azimuth of roughly 120° ; for example, this could be due to vertical fractures aligned parallel to the 30° azimuth. Velocity variations in the vertical plane (axial measurements and 45° P-wave CVA) indicate a less simple symmetry. If the core sample anisotropy was in fact TI, the 45° P-wave CVA data should show a similar $\cos 2\phi$ variation. Figure 5 (a,ii) shows that this is not the case.

The misfit of the modeled velocities from the measured data is presented in Table 1. A good fit to the horizontal CVA data is achieved for models with vertical fractures aligned along an azimuth of 30° (model 3). This fit is further improved by the addition of inclined ellipsoidal vugs dipping downward from roughly 180° to 0° (model 1), as observed in the sample. A model with aligned vugs alone (model 4) is clearly not valid, as it shows a large misfit with the data (Table 1). Likewise, a model with fractures perpendicular to the direction of vug alignment (the natural *in situ* fracture orientation) does not fit the data (model 5). Fitting models to the 45° CVA P-wave data is less successful. These data are of poorer quality than the 0° CVA data and show some strong attenuation effects near the larger vugs. Measurements near the 300° azimuth are taken with a transducer near the large vug at the bottom of the sample (see Figure 2). It is therefore thought that the observed low velocities near 300° (Figure 5) are more likely to be caused by attenuation than by anisotropy. Attenuation effects notwithstanding, there appears to be strong asymmetry in the 45° P-wave measurements, which appears to be best reproduced by a model containing subvertical drilling-induced fractures and inclined aligned ellipsoidal vugs (model 2) (see Figure 5 and Table 1).

Although there are some differences between the model-based and observed velocities, there is a good overall agreement for the first and second models. The second model provides a better fit to the 45° P-wave data, and the first model gives a better fit to the horizontal CVA data. Since the horizontal CVA data are of much better quality, this is taken as a stronger

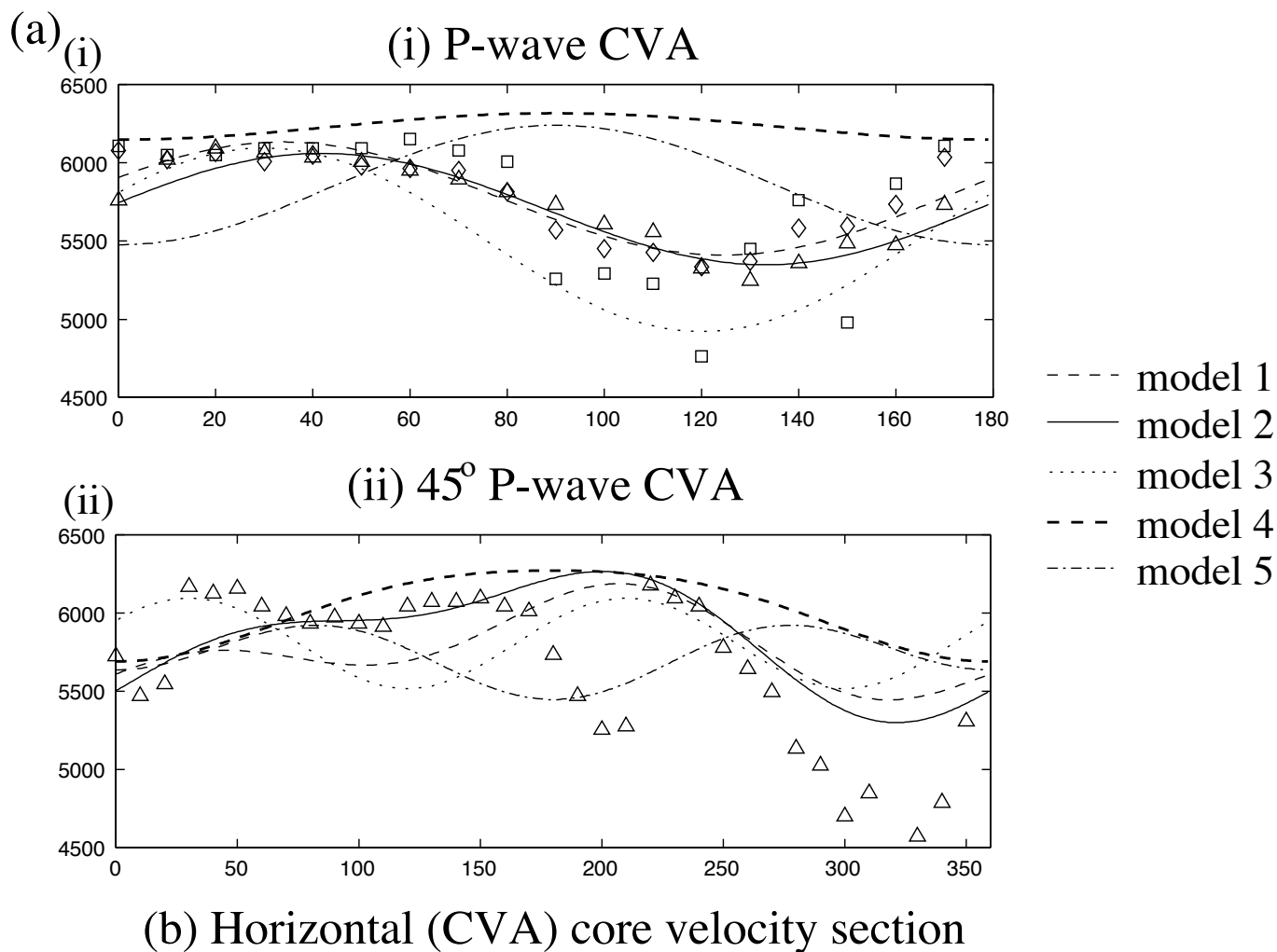


Figure 5: Comparison of measured CVA data and predicted velocities from a range of effective medium models (see Table 1). (a) P-wave CVA at the top (Δ), middle (\diamond) and bottom (\square); (b) and (c) predicted q - S_1 and q - S_2 plotted against S_h CVA for top (Δ) and middle (\diamond) (the shear-wave data was not rotated into true fast and slow orientations); (d) 45° P-wave CVA (Δ).

	model 1	model 2	model 3	model 4	model 5	Isotropic
Fractures	dip=90° strike=30°	dip=80° strike=30°	dip=90° strike=30°	x	dip=60° strike=270°	x
vugs	dip=30° strike=90°	dip=50° strike=80°	x	dip=30° strike=90°	dip=30° strike=90°	x
P-Top	1.69	1.28	5.25	10.04	7.46	6.17
P-Middle	1.66	2.79	5.58	9.38	8.14	6.63
P-Bottom	4.83	5.28	6.00	11.76	10.65	8.81
Sh-Top	12.84	13.00	12.72	15.26	13.00	12.18
Sh-Middle	7.61	7.88	7.95	9.48	8.55	9.97
P-45	9.20	8.33	10.03	11.63	10.74	10.23
RMS	7.49	7.50	8.37	11.44	9.94	8.55
Plot	-----	-----	----	-----	x

Table 1: Summary of effective medium models plotted in Figure 5 with the RMS misfits of each model from the data; given as a percentage of the average velocity of the relevant data. The final values given are the RMS misfits of all the measurements and the last row in the table indicates the line style used for plotting in Figure 5.

constraint on the model fitting. Thus, we deduce that the anisotropy of the core sample is best explained by the combined effects of aligned subhorizontal ellipsoidal vugs and aligned vertical micro-fractures (drilling induced); this results in monoclinic symmetry. We infer that the natural *in situ* fractures (visible in Figure 2) do not contribute to the anisotropy, as they are too widely spaced to generate an effective anisotropy in these ultrasonic measurements. Better constraining the anisotropy would require further lab measurements (for example, rotating the S-wave transducers into the fast and slow shear wave directions).

4 Modelling the surface seismic AVOA response

Using the insight gained into the anisotropy of the core sample, we can now model the effect of fracture- and vug-induced seismic anisotropy on surface seismic measurements. Specifically, we are interested in the potential for using AVOA effects to assess fracture and inclusion related anisotropy. The effective medium approach of the previous section is used, but, in keeping with what we think the *in*

situ conditions are, we model horizontally aligned vugs and vertical fractures (obviously the drilling-induced fractures which contributed to the core sample anisotropy are not present in the reservoir). Thus the assumed reservoir anisotropy has an orthorhombic symmetry. Potential anisotropy due to subseismic scale layering has not been included in these models.

AVOA analysis can provide significant information about the nature and orientation of aligned vertical fractures (e.g., Lynn et al., 1996; MacBeth et al., 1999; Hall et al., 2000). The AVOA signature is influenced by the overall rock properties and so is sensitive to the presence of horizontally aligned vugs. AVOA could therefore potentially provide a useful tool for determining the orientation of the fracturing and identifying highly productive zones containing vertical fractures and aligned vugs.

The effective elastic model derived from the core was determined by using measurements made at conditions different from those *in situ*. The wave frequencies used in the lab are much higher than those of surface seismic, thus the response of the medium may be different, and upscaling to accurately predict such differences will be very difficult. It is noted that while aligned natural fracturing is observed in the core sample, it does not appear to contribute to the anisotropy observed in the ultrasonic data. As noted, the *in situ* fractures are evident in the core sample from oil staining and recrystallisation. Confining pressures may change the aspect ratio of the fractures somewhat, but we do not expect this to change our conclusions significantly. The drilling induced fractures will obviously not be present in the reservoir. It is also noted that the ellipsoidal vugs occur over a large scale-range (micrometers to meters) therefore it is reasonable to assume that the anisotropy induced by the aligned vugs is likely to have an equivalent effect on wave propagation over a range of frequencies. Thus the *in situ* fractures are considered to produce TI anisotropy with a horizontal symmetry axis and the aligned vuggy porosity is assumed to produce TI anisotropy with a verti-

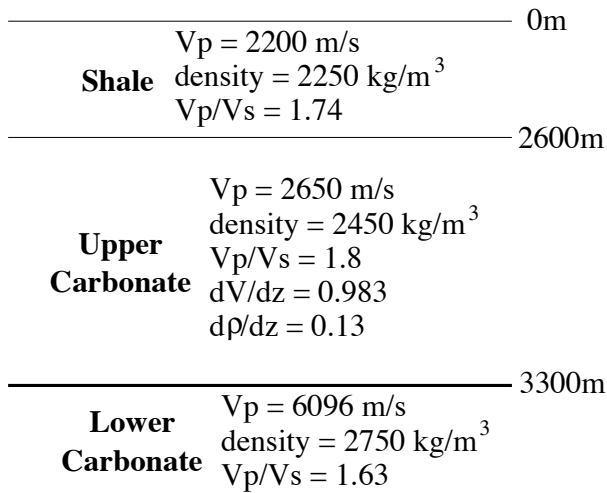


Figure 6: Model used for AVOA analysis. The target reflector is the top of the lower carbonate.

cal symmetry axis. If one or both of these features exist in the subsurface, it may be possible to detect their presence through observations of seismic anisotropy. Our model is only qualitatively thought to represent the actual reservoir anisotropy. Fluid flow between different parts of the pore space (e.g., fractures to vugs) will modify the response of the fractured-vuggy medium to an applied stress. However, this should not alter the symmetry of the system but will likely increase the degree of observed anisotropy, since the fractures will be more compliant. Thus the predicted AVOA effects could be lower than those actually observed.

This section initially considers the azimuth and offset variations in the P-wave reflection coefficient for the reflection from the top of the reservoir. Impedance characteristics consistent with those derived from logs of local wells are used (see Figure 6). P-to-S converted reflections are also investigated, as previous studies have shown that converted phase and shear-wave AVOA can be more sensitive to the fracture character and orientation at near offsets (Hall and Kendall, 1997; Li, 1998).

Figure 7 shows the AVO response, for different azimuths relative to fracture strike, for a model with

Model	Azimuth (degrees)	Critical angle (degrees)
Isotropic	-	33.7
Fractured	0.0	36.6
	18.0	36.6
	36.0	36.6
	54.0	35.6
	72.0	34.2
	90.0	33.7
Fractures and vugs	0.0	33.7 33.2
	18.0	32.7
	36.0	31.7
	54.0	30.7
	72.0	30.2
	90.0	30.2

Table 2: Summary of the critical angles (in degrees) predicted for P-waves incident at the upper/lower carbonate boundary for different azimuths from the fracture normal direction. Fractures are HTI and vugs VTI.

aligned vertical fractures, a model with both vertically aligned fractures and horizontally aligned vugs and the isotropic case. In the anisotropic models, P-wave amplitude versus azimuth (AVAz) effects are only apparent for incident angles beyond 25°. The P-wave critical angle clearly depends on azimuth. This critical angle is marked by sharp peaks in reflection strength. The inclusion of vertical fractures increases the critical angle, but the subsequent addition of horizontally aligned vugs reduces this angle (see Table 2). In general, the critical point moves to further offsets with increase in the angle of wave propagation with respect to the fracture strike. The P-S converted reflection also shows AVAz effects but additionally shows a reversal in polarity of the reflected wave. The offset of this reversal varies with azimuth with respect to the fracture orientation, a diagnostic which may be visible in high-quality data.

Figure 8 presents the AVOA in the azimuth-offset domain (determined using the ray-tracing software, ATRAK; Guest and Kendall, 1993), as would be observed with real data, and provides a comparison be-

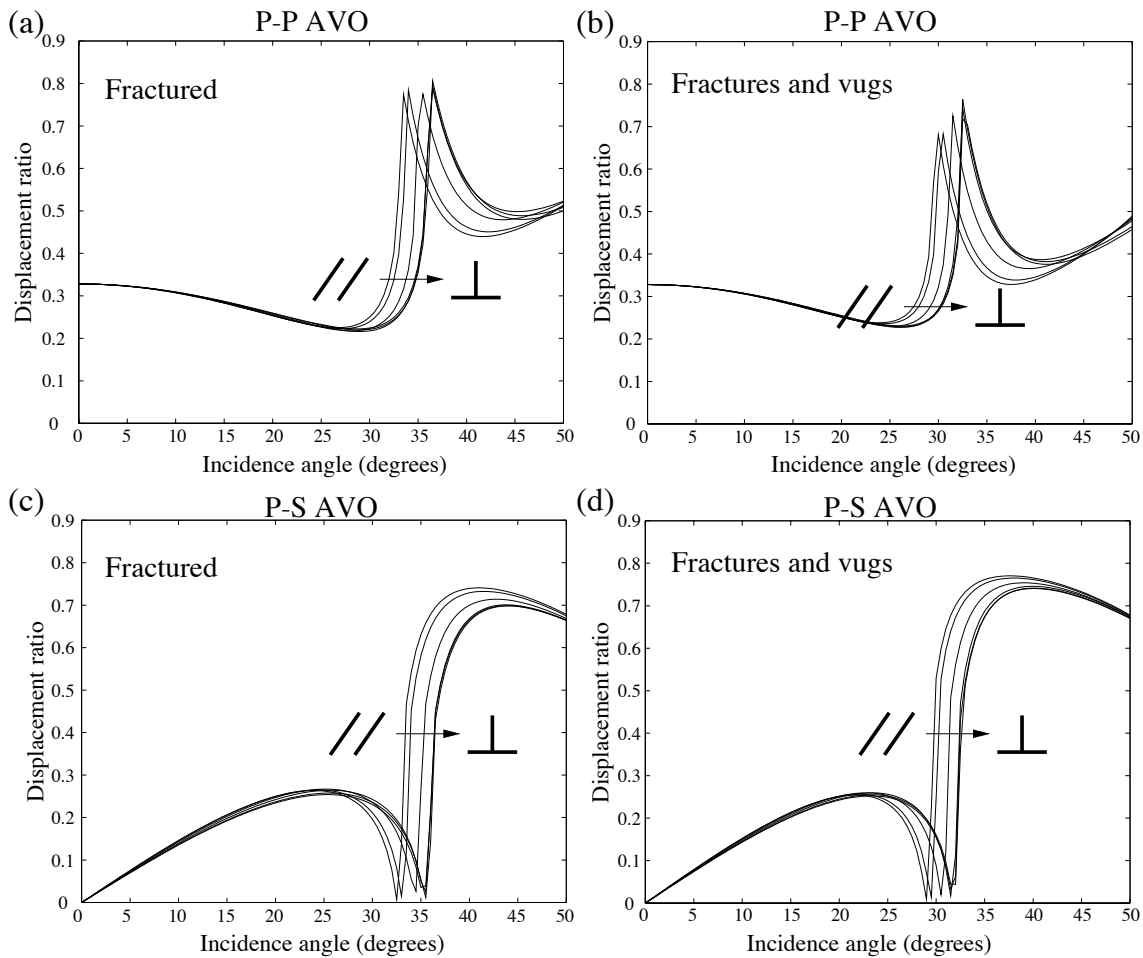


Figure 7: Predicted AVO curves for reflection at the interface between the upper and lower carbonates at azimuths of 0° (fracture parallel, //), 18° , 36° , 54° , 72° , and 180° (fracture perpendicular, \perp) with respect to the fracture strike; (a) and (b) show the P-P AVO whilst (c) and (d) present the AVO for the converted phase reflection of P to S at the reflector. (a) and (c) are for a model with just vertically aligned fractures in the lower carbonate. (b) and (d) are for a model where the lower carbonate contains vertical fracturing and aligned, horizontal, ellipsoidal vugs. The vertical axes show the ratio of the displacement amplitudes of the incidence wave versus the reflected wave.

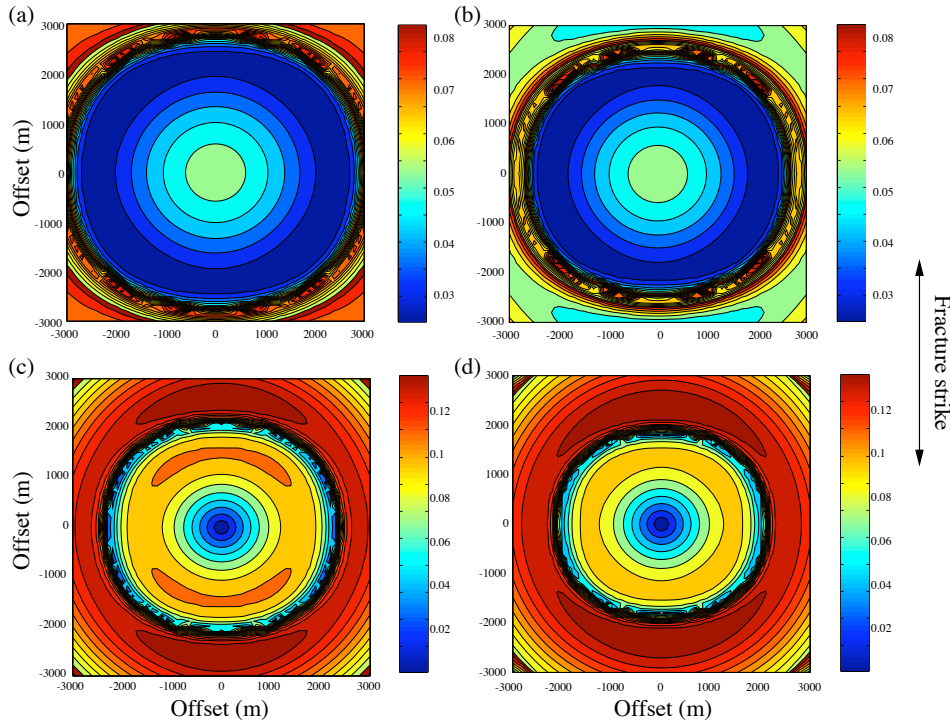


Figure 8: AVOA contour plots for, (a) and (b), P-P reflections, (c) and (d), converted P-S reflections at the top of the lower carbonate with (a) and (c) aligned, vertical fractures or (b) and (d) vertical fractures and horizontal vugs.

tween P-wave and P-S AVOA for the reflection at the top of the carbonate. As indicated above, there is very little variation in the P-wave AVOA, except that the critical reflection moves to further offsets in directions more perpendicular to fracturing. The two cases – fractures alone and fractures with vugs – are differentiated only by the offset at which critical reflections are observed.

Figures 8 (c) and (d) show the AVOA for the reflected P-S conversions. At near offsets, amplitudes of P-S reflections are generally higher than those of P-P reflections. These plots show that the highest reflection amplitudes appear in directions parallel to fracture strike. Additionally, in comparison with P-P, the P-S reflections show clearer differences between the two models. Therefore the P-S AVOA appears to provide a better indication of the fracture orientation at shorter offsets and may also provide a tool for distinguishing between the two models.

These observations indicate that, for this model, P-S AVOA will provide a clearer indication of fracture orientation at near offsets, whereas the P-P AVOA indicates fracture strike only at longer offsets. Both P-S and P-P AVOA may also have potential for distinguishing between the model with fractures alone and the model with fractures and aligned vugs, but the P-P data require offsets near points of critical reflection.

5 Discussions and conclusions

Variations in ultrasonic velocity measurements on a whole-core carbonate sample from the Gulf of Mexico can be explained by seismic anisotropy with a monoclinic symmetry. An effective medium approach has been used to model the effective elasticity of the core sample, which is thought to be anisotropic due to the combined effects of aligned

ellipsoidal vugs and aligned fractures. A number of potential models were tried on the basis of observed fracturing and vug alignment in the sample. Although there are some differences between the predictions from effective medium modeling and the measurements, there is a good overall agreement for a model where the anisotropy is due to a subhorizontal vug alignment with subvertical/vertical, aligned micro-fractures. Further lab measurements (for example, rotating the S-wave transducers into the fast and slow shear wave directions) would help better constrain the core-sample anisotropy. The fractures which induce the anisotropy in the core are drilling induced and not natural fractures. The natural fractures observed in the core sample are too widely spaced to produce an effective anisotropy for ultrasonic core measurements. However, these natural fractures are taken to be indicative of a preferred orientation of *in situ* fractures which produce effective anisotropy for long wavelengths.

For the reservoir models considered here, P-wave AVOA at near offsets is not very sensitive to the fracture orientation. However, at far offsets, the onset of critical reflections varies with azimuth. The inclusion of vertical fractures has the effect of increasing the critical angle and the subsequent addition of horizontally aligned vugs reduce this angle. The critical point moves to further offsets as the direction of wave propagation becomes more oblique to the fracture strike. It is not clear at this stage how viable the detection of such azimuthal variations in critical angle is in actual field surveys, but ocean bottom technology makes acquiring long offsets an easier goal.

Investigation of P-S AVOA showed that, at near offsets, the fracture orientation could be much better determined using converted-wave data. Higher amplitudes are observed in the direction of fracturing and the variation with azimuth of P-S AVO is greater than that for P-waves. P-S AVOA may also hold more potential for distinguishing the highly productive zones of fractures and vugs from zones with fractures alone. Observations of P-wave critical angles and P-S polarity reversals may also be used to

distinguish between these models.

It is likely that fluid-flow effects are significant in situations in which fractures intersect the bands of vuggy porosity (fluid flow will otherwise be negligible, as the matrix permeability is very low in this reservoir). Flow between fractures and vugs has not been accounted for in our modeling but is likely to accentuate the observed anisotropy for the *in situ*, fractured vuggy model. The core measurements were made on a dry sample, so fluid-flow effects in the ultrasonic data were not a factor.

It is important to note that our conclusions are highly model-dependent, and Hall and Kendall (2000, this issue) present a more comprehensive discussion of the sensitivity of P-, S- and converted-wave AVOA to fracturing. Nevertheless, our results suggest that as data quality and coverage improve, spatial variations in fracturing and porosity may be more easily discernible using observations of anisotropy.

Acknowledgments

We would like to thank Luc Ikelle for his efforts in putting together this IWSA volume. Reviews by Prof. Klaus Helbig and an anonymous reviewer helped improve the manuscript. Amoco is acknowledged for permission to publish this work.

References

- Backus, G.E., 1962, Long-wave elastic anisotropy produced by horizontal layering: *J. Geophys. Res.*, 67, 4427-4440.
- Crampin, S., 1993, A review of the effects of crack geometry on wave propagation through aligned cracks: *Can. J. Expl. Geophys.*, 29, 3-17.
- Guest, W.S., and Kendall, J-M., 1993, Modeling seismic waveforms in anisotropic inhomoge-

- neous media using ray and Maslov asymptotic theory: applications to exploration seismology: *Can. J. Expl. Geophys.*, 29, 78-92.
- Hall, S.A., 2000, *Rock fracture characterisation and seismic anisotropy: Application to ocean bottom seismic data*, PhD dissertation, University of Leeds, pp.183.
- Hall, S.A., and Kendall, J-M., 2000, Constraining the interpretation of AVOA for fracture characterisation: *Proceedings of the 9th Internat. Workshop of Seismic Anisotropy*, this issue.
- Hall, S.A., and Kendall, J-M., 1997, Converted phase AVOA effects over multiple fracture sets: application to ocean bottom surveys: 67th Internat. Mtg., Soc. Explor. Geophys., Expanded abstracts, 1195-1198.
- Hall, S.A., Kendall, J-M., Barkved, O.I. and Mueller, M.C., 2000, Fracture characterisation using P-wave AVOA in 3D-OBS data: In *70th Annual Internat. Mtg., Soc., Expl. Geophys., Expanded abstracts*.
- Horne, S., MacBeth, C., Queen, J., Rizer, W. and Cox, V., 1997, Fracture characterisation from near-offset VSP inversion: *Geophys. Prosp.*, 45, 141-164.
- Hudson, J.A., 1981, Wave speeds and attenuation of elastic waves in material containing cracks: *Geophys. J. Roy. Astr. Soc.*, 64, 133-150.
- Kendall, R.R., and Kendall, J-M, 1996, Shear-wave amplitude anomalies in south-central Wyoming: *Leading Edge*, 15, 913-920.
- Li, X.Y., 1998, Processing PP and PS waves in multicomponent sea-floor data for azimuthal anisotropy: Theory and overview: *Proc. 8th Int. Workshop Seismic Anisotropy*, *Rev. Inst. Fr. Pet.*, 53, 607-620.
- Lynn, H. B., Simon, K. M., Bates, C. R., and Van Dok, R., 1996, Naturally fractured gas reservoir's seismic characterization: 66th Internat. Mtg., Soc. Explor. Geophys., Expanded abstracts, 1360-1363.
- MacBeth, C., Jakubowicz, H., Kirk, W., Li, X.Y., and Ohlsen, F., 1999, Fracture-related amplitude variations with offset and azimuth in marine seismic data: *First Break*, 17, 13-26.
- Mueller, M. C., 1991, Prediction of lateral variability in fracture intensity using multicomponent shear-wave surface seismic as a precursor to horizontal drilling in the Austin Chalk: *Geophys. J. Int.*, 107, 409-415.
- Schoenberg, M., and Sayers, C.M., 1995, Seismic anisotropy of fractured rock: *Geophysics*, 60, 204-211.